Proc. Natl. Acad. Sci. USA
Vol. 77, No. 6, pp. 3331–3335, June 1980
Biochemistry

Attenuation and processing of RNA from the *rplJL–rpoBC* transcription unit of *Escherichia coli*

(RNA polymerase/ribosomal proteins/RNase III/RNA·DNA hybrids)

GERARD BARRY, CRAIG SQUIRES, AND CATHERINE L. SQUIRES

Department of Biological Sciences, Columbia University, New York, New York 10027

Communicated by Masayasu Nomura, March 21, 1980

ABSTRACT **Attenuation and processing of the mRNA from the ribosomal protein-RNA polymerase operon *rplJL–rpoBC* have been demonstrated by the analysis of nuclease S1-resistant RNA·DNA hybrids. These hybrids were formed between RNA produced *in vivo* and specific DNA restriction fragments which span the *rplL–rpoB* intercistronic region. The 3′ end of the predominant attenuated RNA lies 69 nucleotides beyond the end of the *rplL* gene following sequence features that are similar to those of other known attenuators. The nonattenuated transcript is normally cleaved in the intercistronic region. However, in an RNase III mutant strain, the hybrids corresponding to the cleaved nonattenuated mRNAs disappear and the expected full-sized hybrid is seen. We have localized the cleavage to an area of possible secondary structure in the transcript approximately 200 nucleotides beyond the end of the *rplL* gene. This demonstrates RNase III processing of *Escherichia coli* mRNA. The methods used in this study permit the examination of specific ends of large and complex polycistronic mRNAs. Such experiments should help in understanding how posttranscriptional events influence gene expression.**

The control of expression of the *rplJL–rpoBC* transcription unit, which encodes the ribosomal proteins L10 and L7/12 and the RNA polymerase subunits β and β', is very complex. Although the four genes are transcribed from one major promoter situated before the *rplJ* gene (1–3), transcription of the *rplL* gene can also be initiated from a minor promoter (4). A minor promoter has also been suggested for the *rpoBC* genes (2, 4). In addition, posttranscriptional regulation of ribosomal protein and RNA polymerase expression has been suggested (5).

The presence of an attenuator before the *rpoB* gene was first proposed on the basis of the arrangement of the *rplJL* and *rpoBC* genes and the observation that the ribosomal proteins were present in the cell in greater quantities (molar basis) than the RNA polymerase subunits (6). The relative amounts of transcription from these ribosomal protein and RNA polymerase genes was found to be consistent with this suggestion (7). Furthermore, the nucleotide sequence of the *rplL–rpoB* intercistronic region has been determined (3) and contains a feature similar to known attenuators (8) which might result in termination of a fraction of the transcripts after the *rplJL* genes are transcribed. Physiological evidence for an attenuator before the *rpoB* gene has recently been provided by studies of *rpl-* and *rpo-lacZ* gene fusions (4) but there has been no physical demonstration of an attenuated transcript.

In this study the RNA that originates *in vivo* from the *rplJL–rpoBC* operon was examined by hybridization of the total cellular RNA to purified restriction fragments. The hybrids were treated with nuclease S1 to destroy all single-stranded nucleic acid regions and then were examined on acrylamide gels (9). This approach allows the mapping of the position of the ends of mRNA molecules for specific genes by examining the hybrids formed with selected restriction fragment probes. The attenuated RNA hybrid has been isolated and the sequence at its 3′ end has been examined. We also show a specific effect of RNase III on *E. coli* mRNA. Examination of cells deficient in RNase III indicates that the *rplJL–rpoBC* transcript is subject to processing by this enzyme. The cleavage occurs in a region of possible RNA secondary structure.

MATERIALS AND METHODS

Plasmids and Strains. The plasmids pBR313 and pBR322 were obtained from H. Boyer (10). The *araI–rplJL–rpoB–lacZ* fusion plasmids and pGB218 have been described (4). The plasmid pGB1002 is a hybrid of pBR313 and the *Eco*RI fragment from λ*drif*^{d}18 (11) which spans the *rplL–rpoB* intercistronic region (6). The plasmid pGB212 is a hybrid formed of pBR322 and a partial *Eco*RI digest of λ*drif*^{d}18; this plasmid contains those fragments that carry part of the *rplK* gene, all of the *rplA*, *rplJ*, *rplL* and *rpoB* genes, and part of the *rpoC* gene. *E. coli* strain MC1000 (Δ*lacIPOZY*, *galU*, *galK*, Δ*ara-leu*, *strA*) was obtained from M. Casadaban (12). The *rnc*+ and the *rnc105* isogeneic strains N2076 and N2077 were obtained from D. Apirion (13). All experiments using recombinant DNA were performed in accordance with the guidelines of the National Institutes of Health.

Hybridization Procedure. Plasmid DNA was purified by a lysozyme/detergent method (14). After cleavage with the restriction enzyme the required fragments were purified by high-pressure reverse-phase chromatography on RPC-5 (15). The *Eco*RI fragment that spans the *rplL–rpoB* intercistronic region [*Eco*RI 1.1-kilobase pair (kbp) probe] was purified from pGB1002. The *Hin*dIII fragment which includes part of the *rplJ* and all of the *rplL*, *rpoB*, and *rpoC* genes (*Hin*dIII 10.3-kbp probe) was purified from pGB218 (Fig. 1). The 1.1-kbp *Eco*RI and the 10.3-kbp *Hin*dIII fragments used in this work are those designated 1.0-kbp and 9.74-kbp in a previous study (4).

RNA was purified from cells in early logarithmic phase by extraction with hot phenol (16). Untransformed cells were grown in L broth; pGB212 transformants were grown in L broth plus ampicillin (20 μg/ml); and *araI–rplJL–rpoB–lacZ* fusion plasmid transformants were grown in preconditioned glycerol L broth plus ampicillin (4). The pGB212 and fusion plasmid transformants (pGBΔB2 and pGB81218) were used to obtain increased amounts of *rpl–rpo* mRNA either by plasmid copy number of by fusion to the *ara* promoter. In the case of these

The publication costs of this article were defrayed in part by page charge payment. This article must therefore be hereby marked "*advertisement*" in accordance with 18 U.S.C. §1734 solely to indicate this fact.

Abbreviations: kbp, kilobase pair(s); bp, base pair(s)

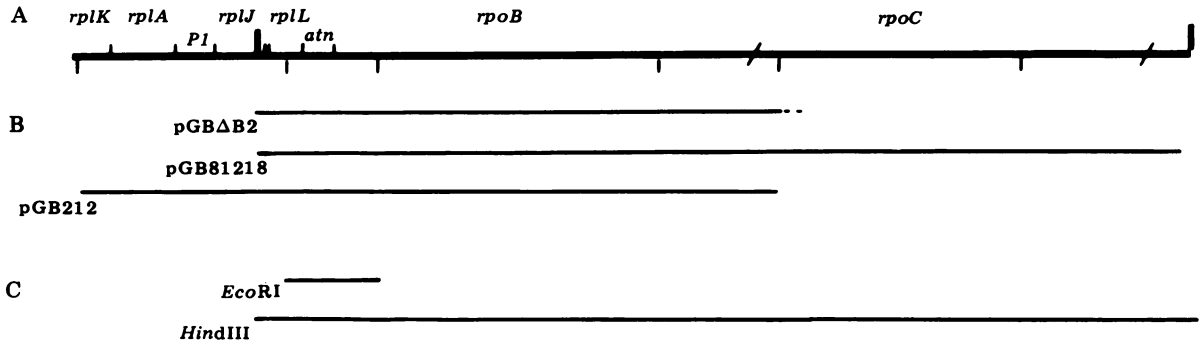

FIG. 1. Structure of hybrid plasmids and DNA probes of the *rplJL-rpoBC* region. (*A*) Genetic and physical maps. The extent of the genes and intercistronic regions are indicated by the short vertical bars above the line; approximate extent is indicated by a diagonal slash. The major promoter and the attenuator are indicated by *P1* and *atn*, respectively. The *Hin*dIII restriction sites are represented by the heavy vertical bars above the genetic map and the *Eco*RI sites, by the vertical bars below the genetic map. (*B*) Physical maps of the DNA segments cloned in the indicated hybrid plasmids. (*C*) DNA probes used in this study and their relationship to the *rplJL–rpoBC* operon. The sizes of the probes are 1.1 and 10.3 kbp, respectively.

fusion plasmid strains, L-arabinose (0.4%) was added to the growth medium one doubling time before the cells were harvested.

The hybridization of RNA and DNA was performed as described (9) with the following changes: 1–2 μg of the *Eco*RI or *Hin*dIII probe and 100 μg of RNA were used per hybridization, the denaturation step used 70°C for 10 min, and the hybrids were formed at 53°C for 3 hr. After nuclease S1 treatment, the hybrids were separated on 5% acrylamide gels and visualized by staining with ethidium bromide.

RNA Sequence Determination. The attenuated RNA hybrid formed with the *Eco*RI 1.1-kbp probe was prepared as described above but with 10 times as much material. The ethidium bromide-stained band was extracted and the 3′ end of the RNA was labeled with [5′-^{32}P]pCp (3000 Ci/mmol; 1 Ci = 3.7 × 10^{10} becquerels; Amersham) (17). Five picomoles of RNA was labeled.

Partial RNase T2 digestions were performed as described (18). Total RNase T1 digestions and two-dimensional separations of oligonucleotides by cellulose acetate electrophoresis and homochromatography on polyetheneimine-cellulose thin-layer plates were carried out as described (19).

RESULTS

Detection of mRNA Ends. mRNA was hybridized to a DNA restriction fragment that spans the *rplL–rpoB* intercistronic region by using conditions favoring RNA·DNA hybrid formation. The hybrids were treated with nuclease S1 and sepa-

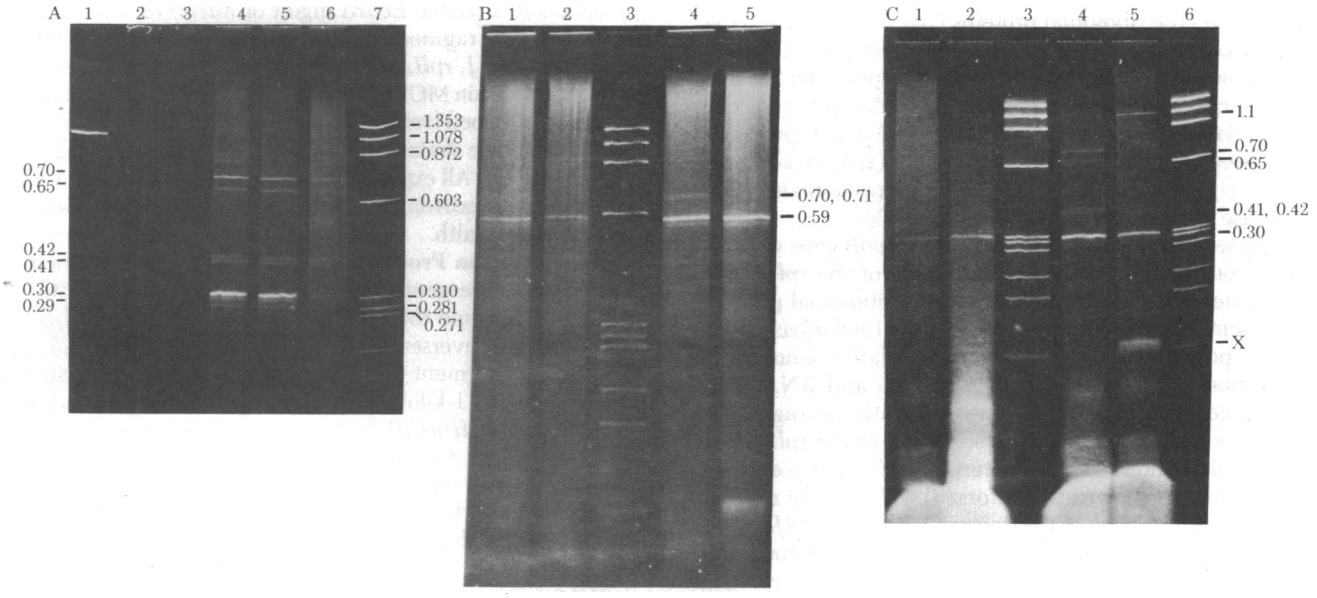

FIG. 2. Analysis of RNA·DNA hybrids by acrylamide gel electrophoresis. (*A*) Hybrids formed between the *Eco*RI probe and RNA from different plasmid transformants. Lane 1 contains a sample of the *Eco*RI DNA probe as a size standard; lane 7 contains the *Hae*III digest of φX174 DNA; sizes are indicated in the right margin in kbp. Lanes 2 and 3 are controls in which DNA alone (the *Eco*RI probe) and RNA alone (same as in lane 4) were subjected to the hybridization and nuclease treatments. Lanes 4, 5, and 6 display the hybrids formed between the *Eco*RI probe and RNA from MC1000 transformed with pGBΔB2, pGB81218, and pGB212, respectively. The sizes of the hybrids are indicated in the left margin in kbp. (*B*) Hybrids formed with the *Hin*dIII DNA probe and RNA from untransformed and transformed *rnc*$^+$ and *rnc*$^-$ sources. Lane 3 contains the φX174 size standards; lanes 1 and 2 contain the hybrids formed with RNA from untransformed *rnc*$^+$ and *rnc*$^-$ sources, and lanes 4 and 5 contain those formed with arabinose-treated pGB81218 transformants of the same strains, respectively. The sizes of the hybrids are indicated in the right margin in kbp. (*C*) Hybrids formed between the *Eco*RI probe and RNA from untransformed and transformed *rnc*$^+$ and *rnc*$^-$ sources. Lanes 3 and 6 contain the φX174 size standards. Lanes 1, 2, 4, and 5 contain the hybrids formed with RNA as in *B*. The sizes of the hybrids are indicated in the right margin in kbp. [The band marked "X" is seen only in *rnc*$^-$ transformants and may be related to RNA associated with plasmid replication (20).]

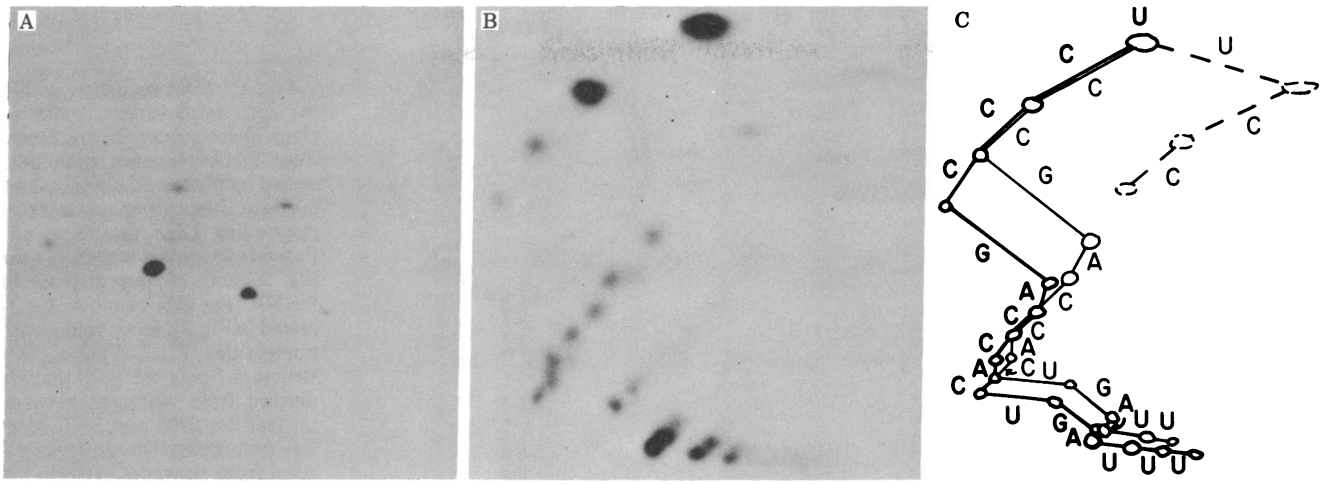

FIG. 3. Nucleotide sequence at the 3′ end of the attenuated mRNA. (*A*) Total RNase T1 digest of attenuated RNA hybrid labeled at the 3′ end with [5′-^{32}P]pCp. The digest was subjected to electrophoresis on cellulose acetate (left to right) followed by homochromatography (bottom to top) on polyetheneimine-cellulose with a 3% homomixture (19). (*B*) Partial RNase T2 digest of labeled attenuated RNA. Cellulose acetate electrophoresis (left to right) was followed by homochromatography (bottom to top) on polyetheneimine-cellulose with a 5% homomixture. (*C*) Tracing of *B* showing the deduced patterns connecting oligonucleotides that retained the terminal -Cp (heavy solid lines) and those connecting oligonucleotides that lost the terminal -Cp (light solid lines). Dashed lines indicate the terminal sequence of the minor RNA component.

rated on acrylamide gels (9). Previous results indicate that levels of enzyme expression (4, 6), as well as mRNA levels (7), are greater for the *rplJL* genes than for the following *rpoBC* genes. If attenuation is the mechanism behind the difference in levels of expression in this operon, we would expect the RNA·DNA hybridization technique to yield two hybrid bands, one the size of the probe and a smaller attenuated RNA band that should be present in approximately 5 times the molar quantity of the probe-sized band (4).

The *Eco*RI 1.1-kbp restriction fragment that spans the *rplL–rpoB* intercistronic region was used to probe transcripts that have ends in this region. We predict a 268 to 271-bp attenuated RNA hybrid on the basis of the position of the attenuator-like structure in the nucleotide sequence. The results obtained with mRNA isolated from strains carrying the *rpl–rpo* genes on plasmids are shown in Fig. 2*A*. The hybrids formed with each RNA were remarkably similar. The major hybrid was approximately 0.30 kbp, close to the predicted size. The apparent absence of a hybrid corresponding to the full-size probe is surprising. Instead, several smaller bands were observed which will be discussed below. Controls were included in which only the RNA or DNA was subjected to the hybridization procedure. The effectiveness of the methods is demonstrated by the complete absence of bands in the control lanes (Fig. 2*A*, lanes 2 and 3).

Location of mRNA Ends. The next set of hybridizations was performed to determine which side of the probe the RNA fragments cover and the approximate location of their ends. RNA was hybridized with the 10.3-kbp *Hin*dIII probe. This probe extends 289 base pairs (bp) to the left side and approximately 8.9 kbp to the right side of the *Eco*RI 1.1-kbp fragment. RNAs that hybridize with the left end of the probes (as drawn in Fig. 1) and end within the intercistronic region will form hybrids 289 bp longer than those formed with the *Eco*RI probe. Similarly, RNAs that hybridize to the right side of the probes will result in hybrids with the *Hin*dIII probe that are much larger than those formed with the *Eco*RI probe. The major 0.30-kbp hybrid, seen with the *Eco*RI probe, was replaced by an equally prominent 0.59-kbp hybrid when the *Hin*dIII probe was used (Fig. 2*B*, lanes 1, 2, 4, and 5). In addition, with the *Hin*dIII probe (Fig. 2*B*, lane 4) a pair of hybrids (0.70 and 0.71 kbp) corresponded to the 0.41- and 0.42-kbp bands seen with the *Eco*RI probe. A number of less-prominent hybrid bands slightly smaller than the presumptive attenuator band also were increased in size (by approximately 0.3 kbp) with the *Hin*dIII probe. This increase in size places these RNAs at the left (*rplL*) side of the *Eco*RI probe and locates the 3′ ends of these RNAs in the intercistronic region. The two prominent 0.65- and 0.70-kbp hybrids (Fig. 2*A*, lanes 4, 5, and 6) obtained with the *Eco*RI probe disappeared when the RNA was hybridized with the *Hin*dIII probe (Fig. 2*B*, lane 4) but a continuum of large hybrids was seen. These hybrids formed from RNAs that have 5′ ends in the *rplL–rpoB* intercistronic region and extend into the *rpoBC* sequences. Presumably, discrete large bands were not observed because the RNA from the *rpoBC* genes was actively degraded and therefore was heterogeneous in size.

Plasmid Amplification Is Not Required to Demonstrate Attenuated mRNA. When strains that did not carry plasmids were used as the source of RNA, the attenuated RNA hybrid was clearly visible. The RNA from such strains gave the same 0.30-kbp hybrid (*Eco*RI probe; Fig. 2*C*, lanes 1 and 2) and 0.59-kbp hybrid (*Hin*dIII probe; Fig. 2*B*, lanes 1 and 2) as obtained with RNA from plasmid-containing strains (Fig. 2*A*, lanes 4, 5, and 6; Fig. 2*B*, lanes 4 and 5; Fig. 2*C*, lanes 4 and 5). Thus, the attenuator can be studied without using plasmids to amplify the mRNA. The plasmids used in this study, however, did increase the concentration of *rpl–rpo* mRNA sufficiently to allow us to observe the nonattenuated RNA.

Nucleotide Sequence at the 3′ End of the Attenuated mRNA. It was of interest to locate the 3′ end of the attenuated mRNA more precisely within the *rplL–rpoB* intercistronic region. We estimate the error of the RNA·DNA fragment size in our experiments at ±15% which, in the case of the 0.30-kbp fragment, places the 3′ end of the RNA 255–345 nucleotides beyond the *Eco*RI restriction site (position 2444) in the *rplL* gene. [The nucleotide numbers used throughout this paper refer to those of the published sequence (3).] It had been shown previously that the attenuated *trp* mRNA ends at more than one position (refs. 19 and 21; unpublished results). We therefore used methods appropriate to the detection and analysis of heterogeneous 3′ ends. We labeled the RNA with [5′-^{32}P]pCp in the presence of RNA ligase and examined this material by using RNase digestions followed by standard two-dimensional electrophoresis/homochromatography techniques.

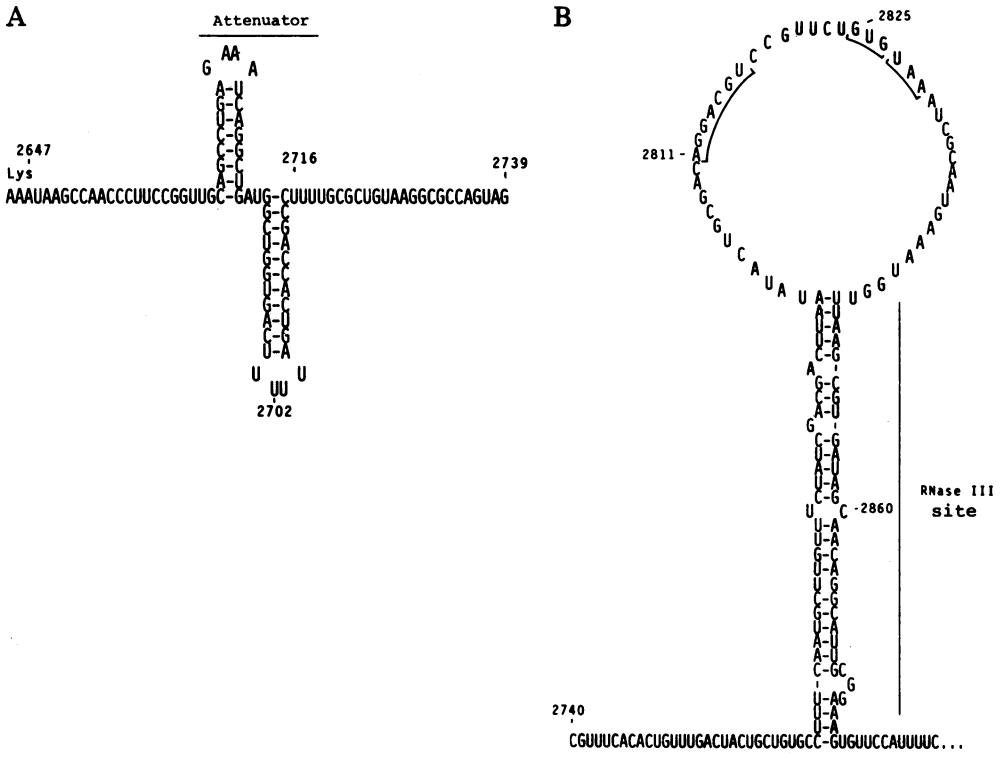

FIG. 4. RNA sequences within the *rplL–rpoB* intercistronic region. These sequences are drawn from DNA sequence data presented by Post *et al.* (3). Numbers indicate the positions in the corresponding DNA sequence. (*A*) Possible secondary structure near the 3′ end of the attenuated mRNA. The RNA sequence suggested in Fig. 3*C* is consistent with nucleotides 2702–2716 of this structure. Spots in Fig. 3*B* that are derived from cleavages between nucleotides 2705 and 2715 occur less frequently than do spots derived from cleavages between nucleotides 2703 and 2705 and nucleotides 2715–2716 (as well as between 2716 and the terminal -Cp residue that is added by RNA ligase and is therefore not shown in this structure). (*B*) RNA sequence in the RNase III-sensitive region. The size of fragments observed in Fig. 2*C* suggests that RNase III cleaves the double-stranded RNA in the vicinity of position 2860.

The results of a total RNase T1 digestion of end-labeled material are shown in Fig. 3*A*. Most of the radioactivity was found in two RNase T1 oligonucleotides: CpCpUp*Cp and CpCpUpUp*Cp (data not shown). This suggests that the RNA in the hybrids ends at the two consecutive uridine residues of the sequence (G)-C-C-U-U. There are two G-C-C-T-T sequences in the intercistronic region (3) which could specify these spots (ending at positions 2717 and 2771). Therefore, additional sequence information must be obtained to distinguish between these two alternative locations.

Fig. 3*B* shows a two-dimensional separation of the products of a partial digestion of the 3′ end-labeled RNA with RNase T2. In addition to the complication introduced by the heterogeneous ends, the interpretation of Fig. 3*B* is also complicated by the fact that some of the bonds in the sequence are more readily cleaved than others, probably as a result of strong secondary interactions. Consequently, the terminal (unlabeled) -Cp residue is attacked by RNase T2 at a higher frequency than are some of the internal bonds. The result is "shadow" spots which correspond to the sequence minus the terminal -Cp residue. Data presented in Fig. 3 are consistent with a segment of the DNA sequence for the intercistronic region. The solid lines in Fig. 3*C* connect spots that correspond to nucleotides 2702–2716 in the DNA sequence (3). The heavy solid lines connect spots containing the terminal (unlabeled) -Cp and the light solid lines connect spots lacking the terminal -Cp. A possible secondary structure for the mRNA in this part of the sequence is shown in Fig. 4*A*. Such a structure helps to explain why some of the bonds in the middle of the sequence are more resistant to cleavage than are bonds in sequences on either side.

Fig. 3 suggests that most of the RNAs from the 0.30-kbp hybrid band end at position 2716, 69 nucleotides after the last amino acid codon of the *rplL* gene. Therefore, the size of the nominal 0.30-kbp hybrid band observed on gels is, in fact, 268 bp. The dashed lines in Fig. 3*C* indicate our interpretation of the second RNA end sequence. Faint spots on the radioautograph suggest that the sequence of the second end is similar to that of the major end displaced by one additional -Up residue. If this analysis is correct, then the minor end terminates at position 2717. It is not known whether the multiple ends that are observed here are the result of *in vivo* termination or degradation or the result of degradation during the isolation procedure. Comparison of these results with those obtained with attenuated RNA from the *trp* operon (refs. 19 and 21; unpublished data) suggests that the true *in vivo* termination point is close to, if not at, the position(s) indicated here.

mRNA Processing. Experiments were carried out to explain the presence of some of the larger bands seen in Fig. 2*A* and to explain why a hybrid corresponding to the nonattenuated mRNA could not be identified. The two pairs of bands first seen in Fig. 2*A* (the 0.41- and 0.42-kbp bands that enter from the left and the 0.65- and 0.70-kbp bands that go to the right) suggest the hypothesis that the probe-length mRNA fragment may be processed by cuts at either of two sites which lie close to each other about 200 nucleotides beyond the end of the *rplL* gene. Left and right halves can be summed to give a size close to that of the *Eco*RI probe (i.e., 0.41 + 0.70 = 1.11 and 0.42 + 0.65 = 1.07). RNase III has been implicated in the processing of phage mRNA (22) and is therefore a candidate to account for the absence of a 1.1-kbp hybrid. The hybrids formed by using RNA from *rnc*$^+$ and *rnc*$^-$ strains containing the plasmid pGB81218 test this possibility. Hybridization of RNA from a transformed strain carrying the *rnc105* mutation with the *Eco*RI probe resulted in a 1.1-kbp hybrid and the loss of the processed RNA hybrids seen with *rnc*$^+$ RNA (Fig. 2*C*, lanes 4 and 5). The attenuated RNA hybrid was unaffected by the difference in RNase III background. The results of these experiments indicate that the nonattenuated RNA is apparent as an intact molecule in RNA isolated from an RNase III mutant source. Fig. 4*B* indicates a region of potential secondary structure in the mRNA that could be the site of the RNase III action we observed. The size of the fragments in Fig. 2*C* indicates that the RNase III processing occurs in the vicinity of position 2860.

DISCUSSION

Comparison of hybrids formed between total *E. coli* RNA and restriction fragment probes of the *rplJL-rpoBC* region has permitted identification of an RNA species that behaves as predicted for RNA attenuated in the *rplL-rpoB* intercistronic region. The prominence of the 0.30-kbp hybrid, over hybrid bands representing more distal sequences, together with the location of the 3′ end of the RNA in the sequences predicted for the attenuator site (4) strongly suggests that this hybrid contains the attenuated RNA.

Attenuation is involved in the regulation of a number of amino acid biosynthetic operons in prokaryotes. Although the sequences responsible for attenuation in the *rplJL-rpoBC* operon have some features in common with these, the control of attenuation of the different classes of operons must differ dramatically. Attenuation in the biosynthetic operons appears to be related to the availability of tRNA species charged with the end product of the particular operon, and this relationship is reflected in the presence of codons for the amino acid in the sequences preceding the attenuator (8). No such simple relationship can be envisioned for the *rpoB* attenuator; this attenuator regulates the synthesis of subunits of RNA polymerase. Although the *rplL-rpoB* attenuator might be responsive to the total levels of charged tRNAs through metabolic regulation (23), the mechanisms by which this might be accomplished are probably not similar to those used by the amino acid biosynthetic operons. Both negative and positive controls have been suggested in the regulation of synthesis of the β and β' subunits (24), and it is possible that at least some of these could act at the attenuator involving RNA polymerase itself and other special regulatory proteins.

Comparison of the hybrids formed between RNA from *rnc*$^+$ and *rnc*$^-$ strains and DNA probes from the *rplJL-rpoBC* operon indicates that the primary transcript of these genes is processed by RNase III. The sizes of the hybrids formed using RNA from *rnc*$^+$ sources suggest that the process point is located in the *rplL-rpoB* intercistronic region in the vicinity of position 2860 (Fig. 4*B*). The sequences in this region (2847–2878) are highly complementary to those at positions 2769–2799, and it is possible that base pairing between these regions forms the double-stranded RNA structure necessary for RNase III cleavage. The involvement of RNase III in the processing of phage mRNA (25) and of rRNA transcripts (26) has been well studied.

The reason for RNase III cleavage of the *rplJL-rpoBC* transcript is unclear. It is possible that some mRNAs are processed even though this may not be necessary for translation. The best-studied role for RNase III is the processing of the early and late polycistronic transcripts of T7 but there is no evidence that this is an essential requirement for translation—e.g., T7 grows on *rnc*$^-$ strains (22, 27). The separation of mRNA for ribosomal proteins from that for RNA polymerase subunits may allow independent expression at the posttranscriptional level as has been proposed for an *rpoC*^{ts} mutant (5).

The RNase III-sensitive structure at the beginning of gene 1.0 in the T7 bacteriophage early transcript contains a number of translation signals (28). These include ribosome binding, translation initiation, and translation termination signals. Such features can also be found in the RNase III-sensitive structure from the *rplL-rpoB* intercistronic region. A sequence of seven bases (A-G-G-A-C-G-U) at position 2811 (Fig. 4*B*) is highly complementary to a region near the 3′ end of 16S rRNA (3′-U-C-C-U-C-C-A-5′), and binding between such complementary regions has been proposed as part of the mechanism of translation initiation (29). This region is followed at position 2825 by an initiation codon (GUG) and a stop codon (UAA). Such an arrangement of translation signals and RNase III sites may have importance in regulation.

Post *et al.* (3) have noted features in the nucleotide sequences of the *rplKA* and *rplJL-rpoBC* operons that might function in their regulation. We have shown that both attenuation and processing by RNase III are associated with prominent secondary structure features in the *rplL-rpoB* intercistronic region. Our observations further support the notion that these sequence features are involved in the modulation of this complex operon.

We thank James Manley for discussing the nuclease S1 treatments and Else Saederup for assisting with the RPC-5 chromatography. We also thank C. Levinthal for the use of the Computer Graphics Facility (Department of Biological Sciences, Columbia University) for analysis of nucleotide sequence information. This work was supported by U.S. Public Health Service Grants GM24751 and GM25178 to C.L.S.

1. Yamamoto, M. & Nomura, M. (1978) *Proc. Natl. Acad. Sci. USA* **75**, 3891–3895.
2. Linn, T. & Scaife, J. (1978) *Nature (London)* **276**, 33–37.
3. Post, L. E., Strycharz, G. D., Nomura, M., Lewis, H. & Dennis, P. P. (1979) *Proc. Natl. Acad. Sci. USA* **76**, 1697–1701.
4. Barry, G., Squires, C. L. & Squires, C. (1979) *Proc. Natl. Acad. Sci. USA* **76**, 4922–4926.
5. Dennis, P. P. & Fiil, N. P. (1979) *J. Biol. Chem.* **254**, 7540–7547.
6. Lindahl, L., Yamamoto, M., Nomura, M., Kirschbaum, J. B., Allet, B. & Rochaix, J.-D. (1977) *J. Mol. Biol.* **109**, 23–47.
7. Dennis, P. P. (1977) *J. Mol. Biol.* **115**, 603–625.
8. Oxender, D., Zurawski, G. & Yanofsky, C. (1979) *Proc. Natl. Acad. Sci. USA* **76**, 5524–5528.
9. Manley, J. L., Sharp, P. A. & Gefter, M. L. (1979) *Proc. Natl. Acad. Sci. USA* **76**, 160–164.
10. Rodriguez, R., Tait, R., Shine, J., Bolivar, F., Heyneker, H., Betlatch, M. & Boyer, H. (1977) in *Miami Winter Symposia*, eds. Scott, W. A. & Werner, R. (Academic, New York), Vol. 13, pp. 73–84.
11. Kirschbaum, J. B. & Konrad, E. B. (1973) *J. Bacteriol.* **116**, 517–526.
12. Casadaban, M. & Cohen, S. N. (1980) *J. Mol. Biol.* **138**, 179–207.
13. Apirion, D. & Watson, N. (1975) *J. Bacteriol.* **124**, 317–324.
14. Meagher, R., Tait, R., Betlach, M. & Boyer, H. (1977) *Cell* **10**, 521–536.
15. Larson, J. E., Hardies, S. C., Patient, R. K. & Wells, R. D. (1979) *J. Biol. Chem.* **254**, 5535–5531.
16. Salser, W., Gesteland, R. F. & Bolle, A. (1967) *Nature (London)* **215**, 588–591.
17. Peattie, D. (1979) *Proc. Natl. Acad. Sci. USA* **76**, 1760–1764.
18. Ziff, E. & Evans, R. (1978) *Cell* **15**, 1463–1475.
19. Squires, C., Lee, F., Bertrand, K., Squires, C. L., Bronson, M. & Yanofsky, C. (1976) *J. Mol. Biol.* **103**, 351–381.
20. Conrad, S. E. & Campbell, J. L. (1979) *Cell* **18**, 61–71.
21. Lee, F., Squires, C. L., Squires, C. & Yanofsky, C. (1976) *J. Mol. Biol.* **103**, 383–393.
22. Dunn, J. J. & Studier, F. W. (1973) *Proc. Natl. Acad. Sci. USA* **70**, 3296–3300.
23. Rose, J. K. & Yanofsky, C. (1972) *J. Mol. Biol.* **69**, 103–118.
24. Scaife, J. (1976) in *RNA Polymerase*, eds. Losick, R. & Chamberlin, M. (Cold Spring Harbor Laboratory, Cold Spring Harbor, NY), pp. 207–225.
25. Rabussay, D. & Geiduschek, E. P. (1977) in *Comprehensive Virology*, eds. Fraenkel-Conrat, H. & Wagner, R. W. (Plenum, New York), Vol. 8, pp. 1–196.
26. Gegenheimer, P., Watson, N. & Apirion, D. (1977) *J. Biol. Chem.* **252**, 3064–3073.
27. Yamada, Y. & Nakada, D. (1976) *J. Virol.* **18**, 1155–1159.
28. McConnell, D. J. (1979) *Nucleic Acids Res.* **6**, 3491–3503.
29. Shine, J. & Dalgarno, L. (1974) *Proc. Natl. Acad. Sci. USA* **71**, 1342–1346.